Plasma-based conversion of CO_2 : current status and future challenges

Reference:

Bogaerts Annemie, Kozák Tomáš, Van Laer Koen, Snoeckx Ramses.- Plasma-based conversion of CO_2 : current status and future challenges

Faraday discussions / Royal Society of Chemistry. Faraday Division [London] - ISSN 1359-6640 - 183(2015), p. 217-232

Full text (Publishers DOI): http://dx.doi.org/doi:10.1039/C5FD00053J

Plasma-based conversion of CO_2: Current status and future challenges

Annemie Bogaerts,* Tomas Kozak, Koen Van Laer and Ramses Snoeckx

DOI: 10.1039/c5d00053

This paper discusses our recent results on plasma-based CO_2 conversion, obtained by a combination of experiments and modeling, for a dielectric barrier discharge (DBD), a microwave plasma and a packed bed DBD reactor. The results illustrate that plasma technology is quite promising for CO_2 conversion, but more research is needed to better understand the underlying mechanisms and to further improve the capabilities.

1 Introduction

The conversion of greenhouse gases (mainly CO_2 and CH_4) into value-added chemicals and liquid fuels is considered as one of the great challenges for the 21st Century [1]. A lot of research is carried out to develop energy-efficient technologies [2-4]. One of these technologies gaining increasing interest is plasma technology.

A plasma is a partially ionized gas, consisting of a large number of neutral species (different types of molecules, radicals and excited species), as well as electrons and various types of ions. These species can all interact with each other, making plasma a highly reactive chemical cocktail, of interest for many applications [5,6].

The great potential of plasma technology for CO_2 conversion is due to the presence of energetic electrons. Indeed, plasma is created by applying electric power to a gas, causing gas breakdown, i.e., the formation of electrons and positive ions (besides other reactive species). As the electrons are much lighter than the other plasma species, they gain most energy from the electric field, and they do not lose their energy so efficiently by collisions with the other plasma species, explaining their higher energy. These energetic electrons can activate the (inert) gas, by electron impact ionization, excitation and dissociation, and the reactive species (i.e., ions, excited species and radicals, respectively) created in this way, will easily undergo other reactions, yielding the formation of new molecules. Thus, the gas itself (e.g., CO_2) does not have to be heated as a whole, but can remain near room temperature. In this way, even strongly endothermic reactions, like CO_2 splitting and dry reforming of methane (DRM), can occur with reasonable energy consumption under mild reaction conditions. However, as the plasma is created by applying electrical power, the energy efficiency of this process is still an important issue.

The most common types of plasmas used for CO_2 conversion are dielectric barrier discharges (DBDs) [7-31], microwave (MW) plasmas [32-37] and gliding arc (GA) discharges [38-45]. The highest energy efficiency was reported for a MW plasma, i.e., up to 90% [32], but this was under very specific conditions, i.e., supersonic gas flow and reduced pressure (~100-200 Torr), and a pressure increase to atmospheric pressure, which would be desirable for industrial applications, yields a dramatic drop in energy efficiency. Indeed, at normal flow conditions and atmospheric pressure, an energy

efficiency up to 40% was reported [6]. A GA plasma also exhibits a rather high energy efficiency, even at atmospheric pressure, i.e., around 43% for a conversion of 18% in the case of CO_2 splitting [45], and even around 60% for a conversion of 8-16%, for DRM [38]. The energy efficiency of a DBD is more limited, i.e., in the order of 2-10% [8-17], but as demonstrated already for other applications [46], it should be possible to improve this energy efficieny by inserting a (dielectric) packing into the reactor, i.e., a so-called packed bed DBD reactor. Moreover, it also operates at atmospheric pressure, and has a very simple design, which is beneficial for upscaling, as has been demonstrated already for the large scale production of ozone [47], and therefore it also has high potential for industrial applications. Finally, when combined with a catalytic packing, it should enable the selective production of targeted compounds [18-23].

Within our research group PLASMANT, we investigate both pure CO_2 conversion [15,48-50] and DRM [16,17], by means of experiments and computer modeling. We have also investigated the effect of adding H_2 or CH_4, as a means to better separate the product gases [24], the effect of adding He or Ar [31], or N_2 [51] which is mostly present in industrial gas flows. Our research up to now was focused on a DBD and a MW plasma. By means of the computer simulations, validated by experiments, we try to elucidate the underlying reaction chemistry, and to investigate how the process can be optimized in terms of conversion and energy efficiency. In this paper, we give an overview of some characteristic, recent results obtained within our group, to illustrate the state-of-the-art of plasma-based CO_2 conversion, and we will also try to identify the most important challenges for the future.

2 Experimental setup

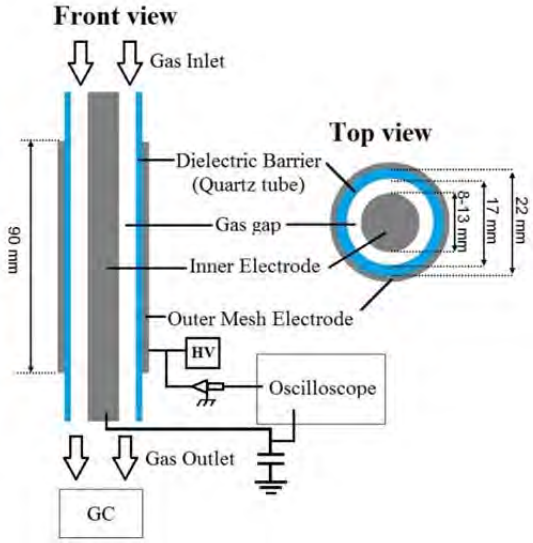

Fig. 1 Schematic diagram of the experimental setup, in front view and top view

The experiments were all carried out in a DBD reactor, of which a schematic drawing is presented in Figure 1. It consists of a central grounded electrode with variable diameter (between 8 and 13 mm), surrounded by a coaxial dielectric tube, with inner and outer diameter of 17 and 22 mm, respectively. The dielectric tube is

covered by a stainless steel mesh, which serves as the outer electrode and is powered by a high voltage power source. The length of this outer electrode is 9 cm, and this defines the length of the plasma zone.

The DBD reactor is coupled to a gas chromatograph to analyse the gas flowing out of the reactor, and to calculate the CO_2 conversion, the yields and selectivities of the formed products, and the energy efficiency, as calculated from the conversion, the power input in the plasma and the gas flow rate (see e.g., [15] for more details).

We performed experiments in a normal (i.e., empty) DBD reactor, as well as in a DBD reactor filled with dielectric packing, i.e., packed bed DBD reactor. For this purpose, we used the smallest rod diameter, yielding a discharge gap (i.e., distance between central electrode and dielectric tube) of approximately 4.5 mm, and a discharge volume of about 15 cm³. We introduced ZrO_2 beads (SiLiBeads), with five different bead size ranges, i.e., 0.90-1.00, 1.00-1.18, 1.25-1.40, 1.60-1.80 and 2.00-2.24 mm diameter.

3 Computational model

We used a zero-dimensional (0D) chemical reaction kinetics model to describe the underlying plasma chemistry of the CO_2 conversion. It consists of solving balance equations for the species densities, based on production and loss rates, as determined by the chemical reactions (see e.g. [16,48] for details).

One balance equation is solved for each species included in the model, i.e., different types of molecules, radicals, ions, excited species, as well as the electrons (see below). These balance equations yield the time-evolution of the species densities, averaged over the plasma reactor volume. Indeed, because it is a 0D model, it only accounts for time-variations, while spatial variations, due to transport in the plasma, are not considered. However, based on the gas flow rate, we can translate the time-variation into a spatial variation, i.e., as a function of distance travelled through the plasma reactor. Besides the species densities, also the average electron energy is calculated, based on an energy balance equation, again with energy source and loss terms as defined by the chemical reactions.

We developed a 0D chemical kinetics model for different gas mixtures relevant for CO_2 conversion, i.e., pure CO_2 [15,48-50], CO_2/CH_4 [16,17] and CO_2/N_2 [51], but here we only show results for pure CO_2. Table 1 gives an overview of the species included in the pure CO_2 model.

Table 1: Overview of the species included in the CO_2 model.

Molecules	Charged species	Radicals	Excited species
CO_2, CO	CO_2^+, CO_4^+, CO^+, $C_2O_2^+$, $C_2O_3^+$, $C_2O_4^+$, C_2^+, C^+, CO_3^-, CO_4^-	C_2O, C, C_2	CO_2(Va, Vb, Vc, Vd), CO_2(V1-V21), CO_2(E1, E2), CO(V1-V10), CO(E1-E4)
O_2, O_3,	O^+, O_2^+, O_4^+, O^-, O_2^-, O_3^-, O_4^-	O	O_2(V1-V4), O_2(E1-E2)
	electrons		

The vibrational levels of CO_2 can play an important role in the CO_2 conversion, depending on the type of plasma to be studied. Indeed, while they are of minor importance in a DBD [48], they are crucial for the CO_2 splitting in a MW plasma [49,50]. This will be illustrated in section 4.2 below. For this reason, we have

developed an extensive chemical kinetics model, taking into account the CO_2, CO and O_2 vibrational levels [49,50]. Hence, the symbols "V" and "E" between brackets for CO_2, CO and O_2 represent the vibrationally and electronically excited levels of these species. Details about these notations can be found in [49,50].

These species will all chemically react with each other. Hence, a large number of chemical reactions are incorporated in these models, including electron impact reactions, electron-ion recombinations, ion-ion, ion-neutral and neutral-neutral reactions. All details about these chemical reaction sets, as well as the corresponding rate coefficients, can be found in [15,48-50].

4 Results and discussion

We present here results, obtained from our experiments and computer simulations, first for CO_2 splitting in a DBD reactor, followed by a comparison of a DBD reactor and a MW plasma, and finally, we will show how the CO_2 conversion and energy efficiency can be improved in a packed bed DBD reactor.

4.1 CO_2 splitting in a DBD reactor

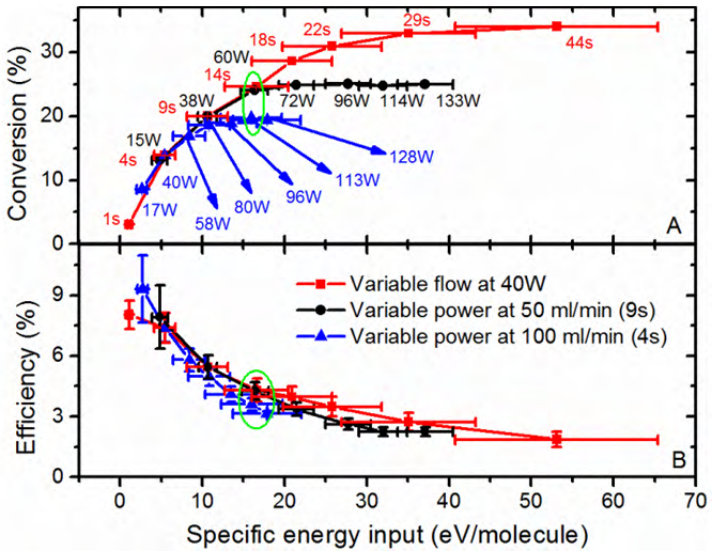

Fig. 2 Measured CO_2 conversion (A) and energy efficiency (B) in a DBD reactor, as a function of the specific energy input (SEI), using alumina dielectrics. The corresponding values of plasma power, resulting in certain SEI values at the fixed gas flow rates of 50 and 100 ml/min (black and blue curves), as well as the corresponding values of the residence time, resulting in certain SEI values at a fixed plasma power of 40 W (red curve), are also shown in (A). The calculation of the error bars is based on the uncertainties of the power, the flow rate and the GC measurements. For the sake of clarity, the error bars are only presented for the energy efficiency. Adopted from [15] with kind permission of Wiley-VCH Verlag.

Figure 2 illustrates the CO_2 conversion and corresponding energy efficiency as a function of the specific energy input (SEI), measured in a DBD reactor. The SEI is the ratio of plasma power over gas flow rate. Therefore, different combinations of power and gas flow rate can give rise to the same SEI. The SEI is typically considered as the major determining factor for the conversion and energy efficiency.

It is clear that the CO_2 conversion rises with SEI, which is logical as more energy is put into the system, either by applying more power for the same amount of gas, or by applying a lower gas flow rate (which corresponds to a longer residence time) at the same power. However, above a certain SEI, the measured conversion seems to saturate, and we did not obtain higher conversion values than 35 % in our experiments. On the other hand, the energy efficiency drops upon increasing SEI, which is also logical, given the formula in section 2 above. Indeed, it is obvious from this formula that when the conversion does not rise to the same extent as the SEI, the energy efficiency will drop.

The highest energy efficiency obtained in this case is 8%, but this corresponds to a very low conversion of only a few %. On the other hand, the highest conversion of 35 % corresponds to a very low energy efficiency of only 2 %. Thus, there is clearly a trade-off between conversion and energy efficiency as a function of SEI.

The values obtained for conversion and energy efficiency are comparable to the data reported in literature for similar conditions (e.g., [7,8]). We can conclude that the obtained CO_2 conversion is reasonable in a DBD reactor, but the energy efficiency is clearly too low for industrial implementation. Indeed, Spencer et al. estimated that if the electrical energy for CO_2 splitting would all originate from fossil fuels, an energy efficiency of 52% would be needed to ensure that more CO_2 can be split in the plasma than the amount of CO_2 created by fossil fuel combustion in the electricity production, needed for sustaining the plasma [52]. When using renewable electricity, this criterion might be somewhat less severe, but still, the energy efficiency is an important issue.

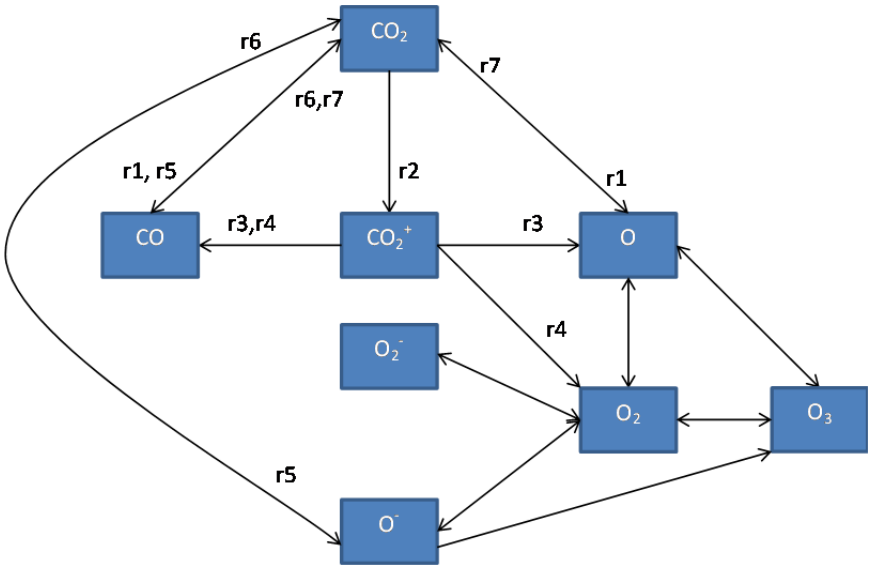

Fig. 3 Chemical reaction scheme, illustrating the chemistry of CO_2 splitting and further reactions between O, O_2 and O_3, as predicted by the model. The labels of the arrows are explained in the text.

Besides the experiments, we have also developed a detailed model for CO_2 conversion in a DBD plasma, to investigate in detail the role of the various processes contributing to the CO_2 splitting [48]. The calculations predict that electron impact dissociation of ground-state CO_2 is the dominant process for CO_2 conversion in a DBD, and the role of the CO_2 vibrational levels is limited in this

case [48] (see more details in section 4.2 below).

Subsequently, the model was extended to calculate the CO_2 conversion in real time [15]. The obtained CO_2 conversion and energy efficiency were in very good agreement with measured data [15]. Therefore, the model can be used to elucidate the underlying reaction paths of CO_2 conversion.

A simplified reaction scheme of CO_2 splitting, as obtained from the model, is illustrated in Figure 3. It is clear that the actual CO_2 splitting is quite straightforward. The most important reactions are electron impact dissociation into CO and O (reaction r1), electron impact ionization into CO_2^+ (r2), which recombines with electrons or O_2^- ions into CO and O and/or O_2 (r3, r4), and electron dissociative attachment into CO and O^- (r5). The created CO molecules are relatively stable, but at long enough residence time, they can recombine with O^- ions or O atoms, to form again CO_2 (r6, r7). This explains, among others, why the CO_2 conversion tends to saturate at high SEI values (corresponding to low gas flow rates or long residence times). At shorter residence times, the O atoms will, however, almost immediately recombine into O_2 or O_3. Moreover, there are several other reactions possible between O, O_2 and O_3, sometimes also involving O^- and O_2^- ions. The details of these reactions are not indicated in Figure 3, but can be found in [15]. These reactions will affect the balance between the formation of O_2 and O_3 as stable products. Our model indeed predicts that the selectivity towards CO formation is always close to 50%, but the selectivity towards O_2 formation varies between 45 and 50%, depending on the O_3 production.

4.2 Comparison of CO_2 splitting in a DBD and MW plasma

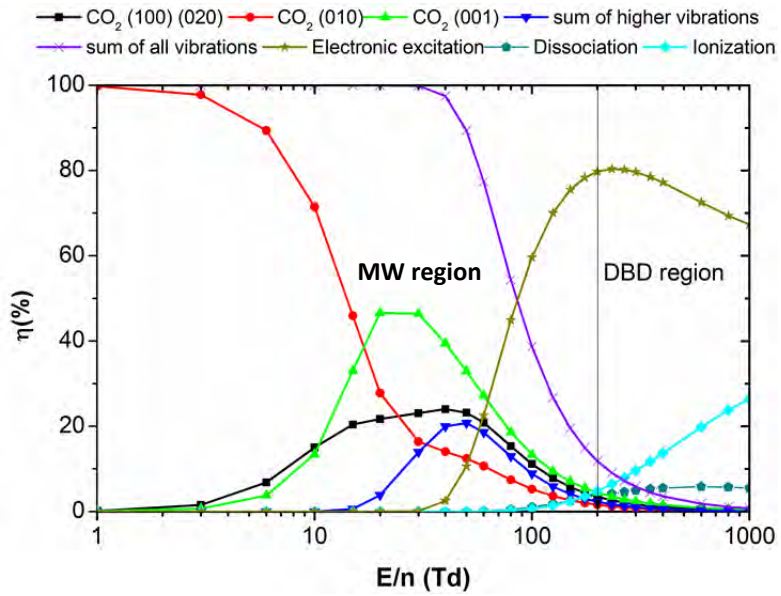

Fig. 4 Fraction of electron energy transferred to different channels of excitation as well as ionization and dissociation of CO_2, as a function of the reduced electric field (E/n), as calculated from the corresponding cross sections of the electron impact reactions. The E/n region characteristic for MW plasmas and DBD plasmas are indicated.

The fact that the energy efficiency for CO_2 splitting is quite limited in a DBD plasma, as mentioned above, is because the reduced electric field is quite high (typically above 200 Td or $200x10^{-21}$ V m²), yielding an average electron energy of 2-3 eV [48], which is somewhat too high for efficient population of the CO_2 vibrational levels [49]. To illustrate this, Figure 4 depicts the fraction of the electron energy transferred to different channels of excitation, ionization and dissociation of CO_2, as a function of the reduced electric field (E/n), as calculated from the cross sections of the corresponding electron impact reactions. It is clear that in the region above 200 Td, indicated as "DBD region", 70-80% of the electron energy goes into electronic excitation, while the remaining 20-30% is used for ionization (increasing with rising E/n) and about 5% goes into dissociation. Note that this electron impact dissociation is also induced by electronic excitation, and thus requires a lot of energy [48]. The fraction of the electron energy going into vibrational excitation is 12% at E/n = 200 Td, but drops quickly upon increasing E/n. Thus, vibrational excitation is of minor importance in the "DBD region".

In a MW plasma, the reduced electric field is typically around 50 Td, which is most appropriate for vibrational excitation of CO_2; see Figure 4. Especially the green curve is important, as this represents the first vibrational level of the asymmetric stretch mode, which is known to provide the most important channel for dissociation [6,49]. Thus, we can deduce already from Figure 4 that a MW plasma will give rise to a high population of CO_2 vibrational levels, which contribute to energy-efficient CO_2 splitting.

Figure 5 shows a comparison of the CO_2 conversion and energy efficiency in a MW plasma and DBD reactor as a function of SEI, as predicted by our model taking into account the CO_2 vibrational levels [49]. Note that the results of the MW plasma are obtained for a reduced pressure of 2660 Pa (20 Torr), as used in the experiments of [33,34], while the DBD results are for atmospheric pressure. Therefore, to compare both discharges, we need to show them at the same SEI in eV/molec, because this is the most fundamental parameter for comparison. Furthermore, the DBD results are obtained at a gas temperature of 300 K, while the MW results are shown both for a fixed gas temperature of 300 K (to allow a more direct comparison with the DBD results, as the rate coefficients of most chemical reactions are a function of gas temperature), as well as for a more realistic gas temperature, self-consistently calculated in the model as a function of time (or distance in the reactor) [50]. In this case, values up to 1000 K are reached; see temperature profile in [50].

It is clear that both the CO_2 conversion and energy efficiency are calculated to be much higher in the MW plasma than in the DBD reactor. The conversion rises as a function of SEI in both cases, which is logical (see also previous section). However, in the DBD reactor, the conversion reaches only about 5%, at an SEI of 3.5 eV/molec, while in the MW plasma with realistic (calculated) gas temperature, the CO_2 conversion is already 12% at an SEI of 2 eV/molec. Note that the calculated conversion in the MW plasma at fixed gas temperature of 300 K is much higher (and thus overestimated), compared to the result at the higher (more realistic) gas temperature. The reason is that the higher gas temperature gives rise to more vibrational-translational (VT) relaxation collisions of the CO_2 vibrational levels, which is the most important loss mechanism for the vibrational population [49,50]. This explains the lower conversion in the case with higher gas temperature. Nevertheless, the CO_2 conversion is still significantly higher than in the DBD reactor operating at 300 K.

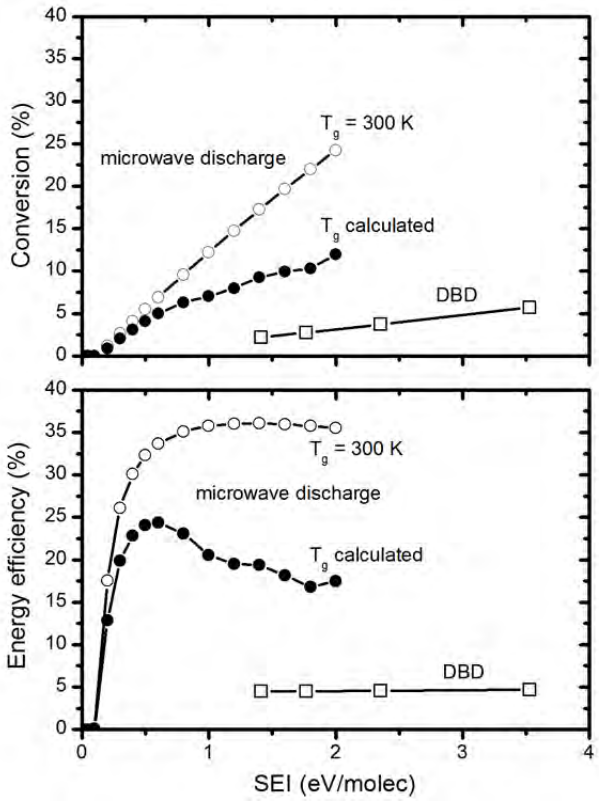

Fig. 5 Calculated CO_2 conversion (top) and energy efficiency (bottom) in a moderate pressure MW discharge and atmospheric pressure DBD reactor, as a function of SEI. The pressure in the MW plasma is 2660 Pa (20 Torr). Calculations are performed for two different gas temperatures, i.e., 300 K, like assumed in the DBD reactor, and a more realistic self-consistently calculated gas temperature as a function of time, reaching values up to 1000 K.

The latter is certainly also true for the energy efficiency, which is calculated to be around 5 % in the DBD reactor (more or less independent from the SEI, as the conversion rises proportionally with the SEI), and it reaches values above 35% (when assuming a constant gas temperature of 300 K; thus overestimated) and around 25% (in the case of the self-consistently calculated gas temperature). In the latter case, the energy efficiency reaches its maximum at an SEI around 0.6 eV/molec, which is in good agreement with the theoretical and experimental results presented in [6], although in that case, energy efficiencies up to 80-90% were reported. Below, we will discuss the major effects that limit the maximum energy efficiency in our case.

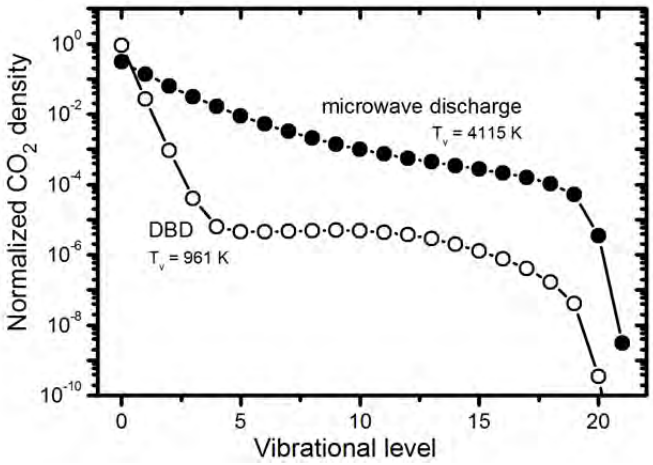

Fig. 6 Normalized vibrational distribution function of the asymmetric mode levels of CO_2 in a moderate pressure MW discharge and an atmospheric pressure DBD plasma, at an SEI of 0.6 eV/molec, both taken at the time of maximum vibrational temperature.

As mentioned above, the reason for the higher CO_2 conversion and energy efficiency in the MW plasma is attributed to the higher population of the CO_2 vibrational levels. This is indeed apparent from Figure 6, where the calculated vibrational distribution function of the CO_2 asymmetric mode levels (i.e., the mode which is most important for CO_2 splitting; cf. above) is plotted, for both the DBD and the MW plasma, for an SEI of 0.6 eV/molec. In the DBD reactor, the population of the vibrational levels drops over several orders of magnitude compared to the ground state density, even for the lowest levels. The corresponding vibrational temperature is calculated to be 961 K. In the MW plasma, the vibrational distribution drops much more smoothly, yielding a vibrational temperature of 4115 K. Although the population of the highest vibrational levels is much lower than the ground state density, they still play an important role in the CO_2 splitting process, which explains the higher CO_2 conversion and energy efficiency. Indeed, while in the DBD reactor, electron impact excitation-dissociation from the CO_2 ground state is mainly responsible for CO_2 splitting (cf. previous section), in the MW plasma, the CO_2 splitting predominantly proceeds by electron impact vibrational excitation of the lowest vibrational levels, followed by vibrational-vibrational (VV) collisions, gradually populating the higher vibrational levels, which then lead to dissociation of the CO_2 molecule. This stepwise vibrational excitation process, or so-called "ladder-climbing" process, is schematically illustrated in Figure 7, and is indeed responsible for the much higher energy efficiency in the MW plasma.

Our model also allows us to identify the discharge conditions that favour the highest energy efficiency for CO_2 conversion. The highest value reached in our calculations, in the case of the realistic gas temperature, was around 32%. This value was obtained at an SEI in the range of 0.4-1.0 eV/molec and a reduced electric field in the range of 50-100 Td [50]. Moreover, our calculations predict that a shorter residence time favours a higher energy efficiency, because in that case the time for VT relaxation, which depopulates the vibrational levels, is longer than the residence time of the gas within the plasma. This corresponds well with the fact that the highest energy efficiencies were reported at supersonic flow conditions [32,35].

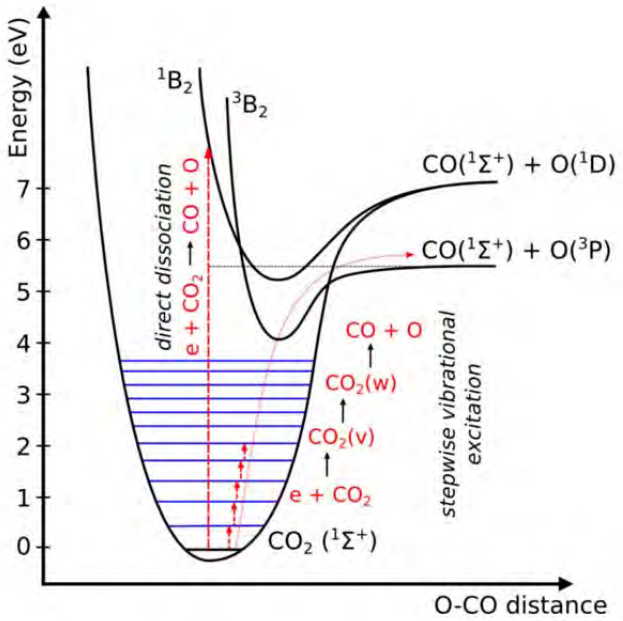

Fig. 7 Schematic diagram of some CO_2 electronic and vibrational levels, illustrating that much more energy is needed for direct electronic excitation-dissociation than for stepwise vibrational excitation, i.e., the so-called ladder climbing process.

The best energy efficiencies obtained experimentally in a MW plasma at moderate pressure were 80% in subsonic flow, and up to 90% in supersonic flow conditions [6,32]. These results were obtained in 1983, and to our knowledge, nobody was able yet to reproduce them since then. However, recently Goede et al. were able to reach energy efficiencies as high as 55% with a MW plasma at moderate pressure and again under supersonic flow conditions [35], which is still higher than the values obtained by our model. Thus, to better understand the limitations in the energy efficiency, we have analysed how the vibrational energy of CO_2 is consumed by individual reactions. Our model predicts that up to 60% of the energy available in the CO_2 vibrational levels can be used for CO_2 dissociation, at least at high enough electron density (order of 10^{20} m^{-3} at a pressure of 100 Torr). The remaining fraction of the energy is largely lost by VT relaxation, which gives rise to the gas heating. Vice versa, because a higher gas temperature gives rise to higher VT relaxation rates, it is desirable to keep the gas temperature as low as possible, to minimize VT relaxation losses in the vibrational population. This is also one of the reasons why the energy efficiency drops upon increasing gas pressure, because of the increasing V-T relaxation processes. One way to reduce this effect is by using a fast gas flow, as mentioned above.

4.3 CO_2 splitting in a packed bed DBD reactor

Finally, we have also investigated whether we can improve the energy efficiency in a DBD plasma, by adding a dielectric packing in the reactor. More specifically, we have inserted ZrO_2 beads, with five different bead size ranges, i.e., 0.90-1.00, 1.00-1.18, 1.25-1.40, 1.60-1.80 and 2.00-2.24 mm diameter, in a DBD reactor with gap size of 4.5 mm.

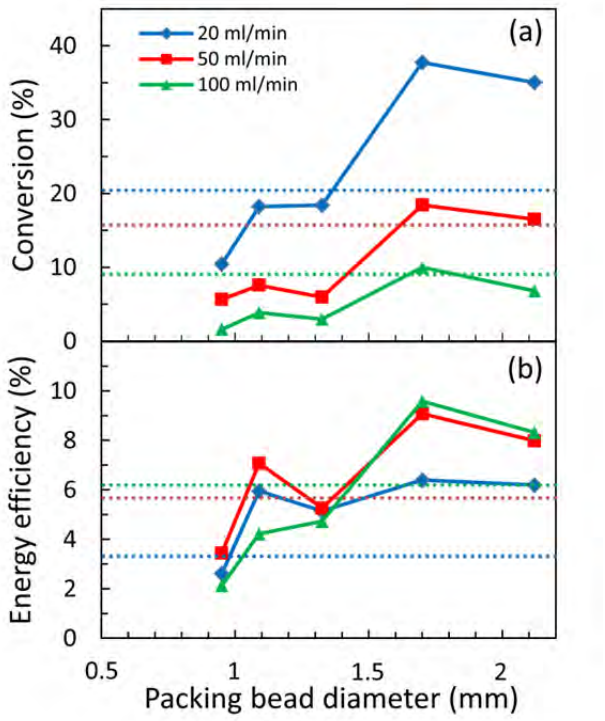

Fig. 8 Measured CO_2 conversion (a) and corresponding energy efficiency (b), as a function of packing bead diameter for ZrO_2, at a power of 60 W and three different gas flow rates. The corresponding results without packing are indicated with dashed horizontal lines.

Figure 8 shows the measured CO_2 conversion (a) and corresponding energy efficiency (b), as a function of bead diameter, for three different gas flow rates, i.e. 20, 50 and 100 ml min^{-1} and an applied power of 60 W. The results are also compared with experiments without packing (dashed horizontal lines), which serve as benchmark, to define the improvement in conversion and energy efficiency.

It is clear that a packed bed reactor can result in a better conversion and energy efficiency than without packing, but only for bead diameters above 1.4 mm. Indeed, the results for lower bead sizes are even worse than without packing. This can be explained because the residence time in the reactor filled with smaller beads is probably too low to benefit from the enhancement effect due to the presence of a packing. The best results, in terms of both conversion and energy efficiency, are obtained for a flow rate of 20 ml/min and a bead diameter of 1.6-1.8 mm. In this case, the conversion reaches 38%, which is almost a factor 2 higher than without packing, while the energy efficiency is 6.4%, which is also nearly a factor 2 higher than without packing. Especially the fact that both conversion and energy efficiency are improved simultaneously is quite promising. The combination of maximum conversion and energy efficiency obtained here, is comparable to or slightly better than the results reported in literature for a packed bed DBD reactor with various types of dielectric materials (silica gel, quartz, α-Al_2O_3, γ-Al_2O_3, $CaTiO_3$ and $BaTiO_3$) at similar conditions [8,25].

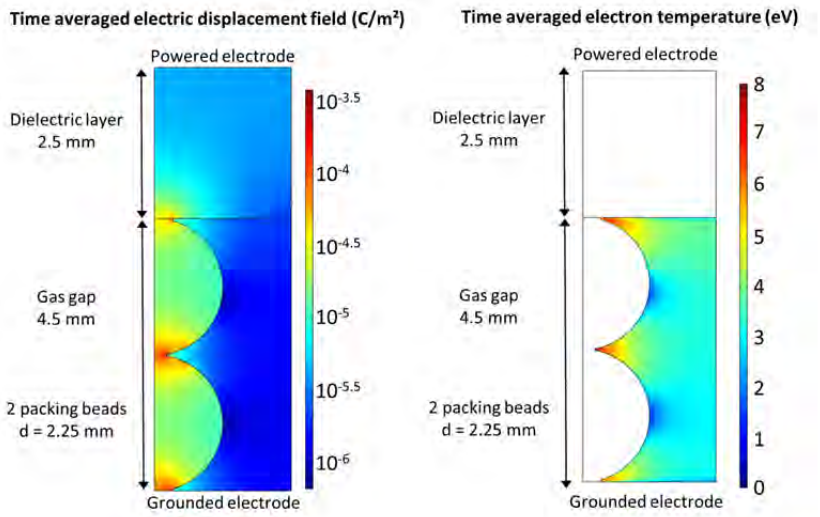

Fig. 9 Calculated time averaged electric displacement field and electron temperature, over one period of the applied potential.

To explain why the packed bed reactor yields a better conversion and energy efficiency, we have developed a 2D fluid model within COMSOL Multiphysics software, for a simplified axisymmetric geometry of a packed bed reactor, consisting of only two beads with diameter of 2.25 mm. This simplified geometry in 2D is needed to keep the simulation time reasonable. Indeed, to resolve the plasma behaviour near the contact points of the beads, a very narrow mesh size is needed (i.e., typically around 50 µm in the bulk, but up to 0.1 µm near the contact points). Thus, the simulation domain contains in the order of 100.000 mesh points, leading to calculation times of a few weeks for a few periods of the applied voltage, even for this simple geometry. Therefore, this model is in first instance developed for a helium plasma instead of a CO_2 plasma, because this yields a more simple plasma chemistry, and it is sufficient to explain the behaviour of the packed bed effect.

Figure 9 illustrates the calculated electric displacement field distribution within the beads and in the plasma and the resulting electron temperature profile in the plasma in this simplified geometry. It is clear that the electric displacement field is much higher near the contact points. This is attributed to polarization of the dielectric material as a result of the applied potential. At the contact points there will thus be local charges of opposite sign close together, which leads to a higher electric displacement field, as well as a locally enhanced electric field in the plasma. The latter gives rise to an enhanced electron temperature for the same applied power. Indeed, the electron temperature is up to 8 eV near the contact points, while it is only 2-3 eV in an empty DBD reactor (or far away from the contact points; see Figure 9). This means that the applied electric power is used more efficiently for heating the electrons, which can then transfer their energy to CO_2 splitting, by electron impact ionization and excitation-dissociation, and this explains the higher CO_2 conversion and energy efficiency, as shown in Figure 8.

5 Conclusion and outlook to future work

We have presented our recent results on CO_2 conversion, obtained by means of combined experimental and computer modeling efforts, for a DBD reactor and a MW plasma. A DBD plasma provides a reasonable conversion, in the order of 30%. However, the corresponding energy efficiency is only in the order of 10%, and this is probably too low for industrial implementation. Indeed, when the electrical energy to sustain the plasma all originates from fossil fuels, it was estimated that an energy efficiency of 52% would be needed for the CO_2 conversion, to compensate for the CO_2 production by the fossil fuel combustion. On the other hand, a DBD plasma is very flexible, as it can easily be switched on and off. Therefore, it has great potential to be combined with renewable energy sources (wind turbines or solar panels), i.e., for the storage of peak renewable energy into chemicals or fuels.

Furthermore, there is still room for improvement in the conversion and energy efficiency of a DBD plasma, by inserting dielectric beads, i.e., in a packed bed DBD reactor, as demonstrated in this paper for ZrO_2. The reason for this higher conversion and energy efficiency is the enhanced electric field near the contact points of the beads, yielding a higher electron temperature, which facilitates electron impact dissociation of CO_2, as could be explained by our model. Moreover, when inserting a catalytic packing in a DBD reactor, the selective production of specific products can be targeted. This was demonstrated already many times in literature for air pollution control (e.g., [46,53-55]), but it has also great potential for CO_2 conversion [18-23]. Nevertheless, we believe that still a lot of research will be needed to find out which catalyst materials are most promising for the selective production of specific compounds.

When comparing a DBD and MW plasma, it is clear that a MW plasma exhibits a much better CO_2 conversion and energy efficiency. This is attributed to the important role of the CO_2 vibrational levels. Indeed, our model calculations have elucidated that the CO_2 conversion proceeds by direct electron impact excitation-dissociation in a DBD plasma, whereas in a MW plasma, the dominant process is electron impact excitation to the lowest vibrational levels, followed by vibrational-vibrational collisions, gradually populating the higher vibrational levels, which give rise to dissociation. As this stepwise vibrational excitation process, or so-called ladder climbing process, requires significantly less energy than direct electron impact excitation-dissociation from the CO_2 ground state, this explains the much better energy efficiency in the MW plasma compared to the DBD reactor.

However, this good energy efficiency is obtained at moderate pressure (order of 3000 Pa), and this was also the case for the experimental data published in literature (e.g., [32,35]). This is not so practical for high-throughput processing of exhaust gases. Increasing the pressure leads, however, to a clear reduction in the energy efficiency [6,36,37], although at atmospheric pressure, a CO_2 conversion of 45% with an energy efficiency of 20% were recently reported [37], which is still better than the results obtained with a DBD plasma.

We also illustrated that computer modelling can contribute to a better insight in the underlying plasma chemistry of CO_2 conversion, and this will be useful for further improving the performance of plasma technology for this application.

To conclude, we believe that plasma technology is very promising for CO_2 conversion into value-added chemicals and new fuels, but still a lot of research will be needed to further improve the capabilities.

Acknowledgments

We thank R. Aerts and W. Van Gaens for setting up the experimental systems and for the interesting results obtained during their PhD study in our group. We also acknowledge financial support from the IAP/7 (Inter-university Attraction Pole) program 'PSI-Physical Chemistry of Plasma-Surface Interactions' by the Belgian Federal Office for Science Policy (BELSPO), the Fund for Scientific Research Flanders (FWO) and the EU-FP7-ITN network "RAPID".

References

Research group PLASMANT, University of Antwerp, Department of Chemistry, Universiteitsplein 1, Antwerp, Belgium. Fax:+32-3-265.23.43; Tel:+32-3-265.23.77; E-mail: annemie.bogaerts@uantwerpen.be

1 S. Solomon, D. Qin, M. Manning, M. Marquis, K. Averyt, M. M. B. Tignor, H. L. Miller and Z. Chen, Eds., Climate Change 2007: The Physical Science Basis. Contribution of Working Group I to the Fourth Assesment Report of the Intergovernmental Panel on Climate Change, Cambridge University Press, New York, 2007

2 G. Centi, E. A. Quadrelli and S. Perathoner, *Energy & Environmental Science*, 2013, **6**, 1711

3 M. Aresta, A. Dibenedetto and A. Angelini, *Chem. Rev*., 2014, **114**, 1709

4 P. Styring, E. A. Quadrelli and K. Armstrong, Carbon Dioxide Utilization: Closing the Carbon Cycle, Elsevier, Amsterdam, 2015

5 A. Bogaerts, E. Neyts, R. Gijbels and J.J.A.M. van der Mullen, *Spectrochim. Acta Part B*, 2002, **57**, 609

6 A. Fridman, Plasma Chemistry, Cambridge University Press, Cambridge, 2008

7 S. Paulussen, B. Verheyde, X. Tu, C. De Bie, T. Martens, D. Petrovic, A. Bogaerts, B. Sels, *Plasma Sources Sci. Technol.*, 2010, **19**, 034015

8 Q. Yu, M. Kong, T. Liu, J. Fei, X. Zheng, *Plasma Chem. Plasma Process.,* 2012, **32**, 153

9 Q. Wang, B.-H. Yan, Y. Jin and Y. Cheng, *Plasma Chem. Plasma Process*., 2009, **29**, 217

10 V. Goujard, J.-M. Tatibouët and C. Batiot-Dupeyrat, *Appl. Catal. A: General*, 2009, **353**, 228

11 X. Zhang and M. S. Cha, *J. Phys. D. Appl. Phys.*, 2013, **46**, 415205

12 X. Tu and J. C. Whitehead, *Appl. Catal. B: Environ*., 2012, **125**, 439

13 Y. Zhang, Y. Li, Y. Wang, C. Liu and B. Eliasson, *Fuel Process. Technol*., 2003, **83**, 101

14 A. Ozkan, T. Dufour, G. Arnoult, P. De Keyzer, A. Bogaerts and F. Reniers, *J. CO_2 Util.*, 2015, **9**, 74

15 R. Aerts, W. Somers and A. Bogaerts, *ChemSusChem*., 2015, **8**, 702

16 R. Snoeckx, R. Aerts, X. Tu and A. Bogaerts, *J. Phys. Chem. C*, 2013, **117**, 4957

17 R. Snoeckx, Y. X. Zeng, X. Tu and A. Bogaerts, *RSC Advances*, 2015, **5**, 29799

18 A.-J. Zhang, A-M. Zhu, J. Guo, Y. Xu and C. Shi, *Chem Eng. J*., 2010, **156**, 601

19 A. Gómez-Ramírez, V. J. Rico, J. Cotrino, A. R. González-Elipe and R. M. Lambert, *ACS Catalysis*, 2014, **4**, 402

20 M. Scapinello, L. M. Martini and P. Tosi, *Plasma Proc. Polym*., 2014, **11**, 624

21 Q. Wang, Y. Cheng and Y. Jin, *Catal. Today*, 2009, **148**, 275

22 Q. Wang, B.-H. Yan, Y. Jin and Y. Cheng, *Energy & Fuels*, 2009, **23**, 4196

23 B. Eliasson, U. Kogelschatz, B. Xue and L.-M. Zhou, *Ind. Eng. Chem. Res*., 1998, **37**, 3350

24 R. Aerts, R. Snoeckx and A. Bogaerts, *Plasma Process. Polym.,* 2014, **11**, 985

25 D. Mei, X. Zhu, Y. He, J. D. Yan and X. Tu, *Plasma Sources Sci. Technol.*, 2015, **24**, 015011

26 J. Wang, G. Xia, A. Huang, S. L. Suib, Y. Hayashi and H. Matsumoto, *J. Catal*., 1999, **185,** 152

27 R. Li, Q. Tang, S. Yin and T. Sato, *J. Phys. D. Appl. Phys.,* 2007, **40**, 5187

28 S. Wang, Y. Zhang, X. Liu and X. Wang, *Plasma Chem. Plasma Process.* 2012, **32**, 979

29 C. De Bie, T. Martens, J. van Dijk, S. Paulussen, B. Verheyde and A. Bogaerts, *Plasma Sources Sci. Technol.,* 2011, **20**, 024008

30 N. R. Pinhao, A. Janeco and J. B. Branco, *Plasma Chem Plasma Proc.*, 2011, **31**, 427

31 M. Ramakers, I. Michielsen, R. Aerts, V. Meynen and A. Bogaerts, *Plasma Process. Polym.*, 2015, **12**, DOI: 10.1002/ppap.201400213

32 R. I. Asisov, V. K. Givotov, E. G. Krasheninnikov, B. V. Potapkin, V. D. Rusanov and A. Fridman, *Sov. Phys., Doklady*, 1983, **271**, 94

33 N. Britun, T. Godfroid and R. Snyders, *Plasma Sources Sci. Technol*., 2012, **21,** 035007

34 T. Silva, N. Britun, T. Godfroid and R. Snyders, *Plasma Sources Sci. Technol*., 2014, **23**, 025009

35 A. P. H. Goede, W. A. Bongers, M. F. Graswinckel, M. C. M. van de Sanden, M. Leins, J. Kopecki, A. Schulz and M. Walker, EPJ Web of Conferences, 3rd Eur. Energy Conference, 2013

36 A. Vesel, M. Mozetic, A. Drenik and M. Balat-Pichelin, *Chem. Phys.,* 2011, **382**, 127

37 L. F. Spencer, A. D. Gallimore, *Plasma Sources Sci. Technol.,* 2013, **22**, 015019

38 X. Tu and J. C. Whitehead, *Int. J. Hydrogen Energy*, 2014, **39**, 9658

39 A. Indarto, D. R. Yang, J.-W. Choi, H. Lee, H. K. Song, *J. Hazard. Mater.,* 2007, **146**, 309

40 A. Indarto, J. Choi, H. Lee and H. K. Song, *Environ. Eng. Sci.,* 2006, **23**, 1033

41 Z. Bo, J. Yan, X. Li, Y. Chi and K. Cen, *Int. J. Hydrogen Energy,* 2008, **33**, 5545

42 Y.-C. Yang, B.-J. Lee and Y.-N. Chun, *Energy,* 2009, **34**, 172

43 N. Rueangjitt, T. Sreethawong, S. Chavadej, H. Sekiguchi, *Chem. Eng. J.,* 2009, **155**, 874

44 C. S. Kalra, Y. I. Cho, A. Gutsol, A. Fridman and T. S. Rufael, *Rev. Sci. Instrum.,* 2005, **76**, 025110

45 T. Nunnally, K. Gutsol, A. Rabinovich, A. Fridman, A. Gutsol and A. Kemoun, *J. Phys. D. Appl. Phys.,* 2011, **44**, 274009

46 H. L. Chen, H. M. Lee, S. H. Chen and M.B. Chang, *Ind. Eng. Chem. Res*., 2008, **47**, 2122

47 U. Kogelschatz, *Plasma Chem. Plasma Process*., 2003, **23**, 1

48 R. Aerts, T. Martens and A. Bogaerts, *J. Phys. Chem. C,* 2012, **116**, 23257

49 T. Kozák and A. Bogaerts, *Plasma Sources Sci. Technol.*, 2014, **23**, 045004

50 T. Kozák and A. Bogaerts, *Plasma Sources Sci. Technol.,* 2015, **24**, 015024

51 S. Heijkers, R. Snoeckx, T. Kozák, T. Silva, T. Godfroid, N. Britun, R. Snyders and A. Bogaerts, *J. Phys. Chem. C,* (in press)

52 L. F. Spencer and A. D. Gallimore, *Plasma Chem. Plasma Process.,* 2011, **31**, 79

53 H. L. Chen, H. M. Lee, S. H. Chen, M.B. Chang, S. J. Yu and S. N. Li, *Env. Sci. Technol.*, 2009, **43**, 2216

54 J. Van Durme, J. Dewulf, C. Leys and H. Van Langenhove, *Appl. Cat. B: Environm*., 2008, **78**, 324

55 H.-H. Kim and A. Ogata, *Eur. Phys. J. Appl. Phys*., 2011, **55**, 13806